Title
Estimate of Rayleigh-to-Love wave ratio in the secondary microseism by colocated ring laser and seismograph

Journal
Geophysical Research Letters, 42(8)

ISSN
0094-8276

Authors
Tanimoto, Toshiro
Hadziioannou, Céline
Igel, Heiner
et al.

Publication Date
2015-04-28

DOI
10.1002/2015gl063637

Estimate of Rayleigh-to-Love wave ratio in the secondary microseism by co-located ring laser and seismograph

Toshiro Tanimoto[1]*, Céline Hadziioannou[2], Heiner Igel[2], Joachim Wasserman[2], Ulrich Schreiber[3], and André Gebauer[3]

1. Department of Earth Science and Earth Research Institute, University of California, Santa Barbara, California 93106, USA.
2. Department of Earth and Environmental Sciences, Ludwig-Maximilians-University, Theresienstr. 41 80333 Munich, Germany
3. Forschungseinrichtung Satellitengeodaesie, Technische Universitaet Muenchen - Fundamentalstation Wettzell, Sackenrieder Str. 25, D-93444 Bad Koetzting, Germany

*Corresponding author: Email toshiro@geol.ucsb.edu

Abstract

Using a co-located ring laser and an STS-2 seismograph, we estimate the ratio of Rayleigh-to-Love waves in the secondary microseism at Wettzell, Germany, for frequencies between 0.13 and 0.30 Hz. Rayleigh-wave surface acceleration was derived from the vertical component of STS-2 and Love-wave surface acceleration was derived from the ring laser. Surface wave amplitudes are comparable; near the spectral peak about 0.22 Hz, Rayleigh-wave amplitudes are about 20 percent higher than Love-wave amplitudes but outside this range, Love-wave amplitudes become higher. In terms of the kinetic energy, Rayleigh-wave energy is about 20-35 percent smaller on average than Love-wave energy. The observed secondary microseism at WET thus consists of comparable Rayleigh and Love waves but contributions from Love waves are larger. This is surprising as the only known excitation mechanism for the secondary microseism, described by Longuet-Higgins [1950], is equivalent to a vertical force and should mostly excite Rayleigh waves.

1. Introduction

One of the outstanding questions on seismic noise (microseism) is how much Rayleigh waves and Love waves are contained in the primary microseism (about 0.05-0.07 Hz) and in the secondary microseism (about 0.10-0.40 Hz). A precise answer to this question is surprisingly difficult because the amount of Love waves is hard to estimate. The main reason is that, while vertical component seismograms record only Rayleigh waves, horizontal component seismograms contain both Rayleigh and Love waves and their separation is not necessarily straightforward.

Nishida et al. [2008] estimated the ratio of Love waves to Rayleigh waves using an array of tilt meters in Japan. Since phase velocities of Rayleigh and Love waves are different, separation of the two types of waves is in principle possible by an array observation. Their conclusion was that there was more Love-wave energy than Rayleigh-wave energy below 0.1 Hz but it changed above 0.1 Hz and Love-wave energy became about 50 percent of Rayleigh-wave energy.

In this study, we take advantage of a unique set of instruments at Wettzell (WET), Germany, where an STS-2 seismograph and a ring laser [Schreiber et al., 2009; Schreiber and Wells, 2013] are co-located. Our basic approach is to estimate the amount of Rayleigh waves from the vertical component seismograph (STS-2) and the amount of Love waves from the ring laser. The ring laser records the rotation and its data consist of pure SH-type waves. For the relatively low frequency range of microseism (0.05-0.5 Hz), surface waves (Love waves) would be dominant in the records.

We describe the general characteristics of the ring laser data in section 2, our stacking approach in section 3 and our results in section 4.

2. Seasonal variation in Love waves in microseism

The ring laser at WET measures the vertical (z) component of rotation rate $\dot{\omega}_z = (1/2)(\nabla \times \mathbf{v})_z$ where the dot denotes time derivative and $\mathbf{v}$ denotes ground velocity. There is a small possibility that tilt can contaminate the data, thus signal related to P-SV type seismic waves (Rayleigh waves) may sneak in, but Pham et al. (2009) showed that the effects of tilt are negligible even for large earthquakes. We also make our own estimate in the discussion. In practice, the data can be considered to be dominated by SH type seismic waves (Love waves).

We analyzed the ring laser data at WET from 2009 to 2014. Fig. 1 shows the power spectral density (PSD) for the frequency band 0.13-0.30 Hz. Each 6-hour long data series was used to get Fourier spectra $F(\omega)$ and the PSD was computed by $|F(\omega)|^2 / T$ where T is the length of time series (six hours). Each point in Fig. 1 (left) corresponds to one 6-hour time interval. Data over the span of five years were folded onto one-year interval using the Julian days. There were points above the maximum PSD value in this figure that were presumably caused by earthquakes but as our goal is to study the microseisms, we focus on the small-amplitude range. Even in the data shown in Fig. 1, there may be some effects from earthquakes, buried in the scatter of points. We specifically use a catalogue of earthquakes to remove these effects later.

The seasonal variation is obvious in the raw PSD data (Fig. 1, left). The monthly means (Fig. 1, right) show that the amplitudes in northern-hemisphere winter are about 10 times larger than the amplitudes in summer. This may not seem surprising as we have seen such seasonal variations in the microseisms. But most past observations were for

Rayleigh waves from vertical component seismographs. Here we confirm the fact that Love waves in the secondary microseism also show very strong seasonal variations.

3. Stacked Spectra

The goal of this study is to estimate the amount of Love waves and Rayleigh waves contained in the microseism. The basic approach we adopt is to create typical spectra for the ring laser data and also for the vertical component data that are as much free from earthquake effects as possible, ideally showing the effects of seismic noise only.

Since data in Fig. 1 show scatter and may contain some effects from earthquakes, we need to proceed carefully. In this study, we decided to focus on relatively small-amplitude time intervals where the effects of earthquakes are more obvious. We initially selected time intervals that had the PSD of 0.001 ($nrad^2$ /s) or less and checked the selected time intervals against the list of earthquakes reported in the Global Centroid Moment Tensor (GCMT) catalogue. We then removed the days of earthquakes from our data set. This processing removed almost all days with earthquakes larger than magnitude 5.5.

For the selected time intervals, we stacked Fourier spectra and came up with the typical (average) spectra of ground velocity for three components (Fig. 2, top) and the spectra for the rotation (Fig. 2b, bottom). One of the most notable features in the rotation spectra is the lack of a clean peak for the primary microseism (0.05-0.07 Hz). The same peaks in horizontal components of STS-2 are sharper, although they are much smaller than the peak in vertical component. Fig. 2 shows that the spectra from the ring laser is generally noisy in comparison to the vertical-component STS-2 spectra and we believe this noise is the reason that the spectral peak for the primary microseism seems to have almost disappeared. Although there still exists a broad peak around 0.05 Hz, the spectral peak for the primary microseism is not clear-cut. Fig. 2 may be interpreted as Rayleigh waves having larger energy than Love waves in the primary microseism, its demonstration will require a good understanding of detailed local structure which we do not have at the moment. In this study, we decided to focus on the secondary microseisms. We will mainly discuss the secondary microseism for the frequency range 0.13-0.30 Hz hereafter.

The peak frequencies in Fig. 2 (top) may appear to be different from previous studies (e.g., Chevrot et al., 2007). This difference is mainly due to the fact that our selected time intervals are from small-amplitude days and thus are somewhat biased to the summer. If we computed spectra for a year, the peak between 0.15 and 0.20 Hz becomes higher. We believe they are all generated in the oceans but the source locations (oceans) differ to some extent in winter and summer. Seasonal variations are seen at all frequencies between 0.13 and 0.30 Hz, thus an alternative explanation (for the peak at 0.22 Hz) by cultural noise does not seem to apply.

4. Conversion to Surface Amplitude and Kinetic Energy

Two spectra in Fig. 2 are in different units and cannot be compared against each other directly. In order to compare them on an equal footing, we convert these data to surface acceleration. Since the vertical-component data from STS-2 are given in ground velocity, a simple multiplication of angular frequency converts the spectra in the top panel in Fig. 2 to vertical acceleration spectra.

For the rotation spectra in the bottom panel, we need a few more steps of processing. We take advantage of the relation that a multiplication of 2C to the rotation spectra, where C is the Love wave phase velocity, converts the spectra to surface transverse acceleration. This relationship was originally pointed out by Pancha et al. [2000] for two earthquakes and extensively used for further analysis by, for example, Igel et al. [2005], Igel et al. [2007], Ferreira and Igel [2009], Kurrle et al. [2010] and Hadziioannou et al. [2012]. This processing assumes that the spectra in the bottom panel consist of the fundamental-mode Love waves only. This assumption was shown to hold for the secondary microseisms (0.1-0.2 Hz) by showing that phase velocity matches that of the fundamental-mode Love waves [Hadziioannou et al., 2012].

In order to apply this approach, we need to know the Love wave phase velocity. In this paper, we rely on an earth model reported by Fichtner et al. [2013], based on the multi-scale waveform inversion for the European continent. Fig. 3a shows their P-wave and S-wave model at WET. It is an anisotropic model and Fig. 3a shows PV, PH, SV and SH velocities. Fig. 3b shows Love-wave phase velocity for this model up to 0.45 Hz. Fig. 3c shows the surface Rayleigh-wave ellipticity that we used to estimate horizontal amplitudes of Rayleigh waves from vertical amplitudes.

Fig. 4a shows comparison between surface amplitudes; the red line is the surface transverse acceleration, obtained by multiplying 2C (Fig. 3b) to the rotation spectra in Fig. 2 (bottom). Blue line is the vertical acceleration obtained from the vertical spectra in Fig. 2 (top). Green line is the surface horizontal amplitude of Rayleigh waves, obtained from the blue line, multiplying by surface ellipticity computed in Fig. 3c.

In Fig. 2, the peak frequency for the rotation spectra (bottom) appears to be shifted toward higher frequency with respect to the peak for the vertical spectra (top). Because phase velocity is frequency-dependent and tends to be faster for lower frequencies, the multiplication by C moves the rotation peak towards the vertical spectra peak as Fig. 4a shows. In other words, the mismatch between the peaks in Fig. 2 is related to the frequency dependence of phase velocity and becomes small when 2C is multiplied to the rotation spectra.

Fig. 4a shows that near the peak range of 0.22-0.23 Hz, Rayleigh-wave vertical acceleration exceeds Love-wave transverse acceleration by about 20 percent. But outside this frequency range, Love wave amplitudes become larger. Therefore, in terms of surface amplitudes, Love waves and Rayleigh waves are basically comparable.

We also converted these surface amplitudes to the kinetic energy of Rayleigh and Love waves. We assumed that the vertical spectra consist of fundamental-mode Rayleigh waves and the rotation spectra consist of fundamental-mode Love waves. Fig. 4c shows an example of the eigenfunction for Love waves (W) and the vertical (U) and the horizontal (V) eigenfunctions of Rayleigh waves at 0.22 Hz, computed for the structure in Fig. 3a. Since SH-SV anisotropy is strong in Fig. 3a (more than 10 percent), we also computed those for an isotropic model (dashed) in order to examine the influence of anisotropy on our results. For the isotropic calculation, velocities were simply averaged at each depth. Close matches between the solid and dashed lines indicate that anisotropy does not change our results.

Using those eigenfunctions, the kinetic energies are computed by $E_L = \omega^2 \int_0^R \rho W^2 r^2 dr$ and $E_R = \omega^2 \int_0^R \rho (U^2 + V^2) r^2 dr$ for Love waves and Rayleigh waves, respectively. The integrated results are plotted in Fig. 4b in blue. In terms of the kinetic energy, the maximum value near 0.22 Hz is now slightly below 1. It shows that Love wave kinetic energy is consistently larger than Rayleigh-wave kinetic energy for the range 0.13-0.30 Hz.

In winter, seismic noise has more energy between 0.15 Hz and 0.20 Hz and thus the peak frequency range of the secondary microseism throughout a year is approximately 0.15-0.25 Hz at WET. If we average these kinetic-energy ratios for this range, we get the Love-to-Rayleigh wave ratio of 0.79. If we average for the whole range in this figure, 0.13-0.30 Hz, we get 0.65. We can thus conclude that there are approximately 20-35 percent more Love-wave energy than Rayleigh-wave energy in the secondary microseism at WET.

5. Discussion

Our analysis relies on an Earth model at WET [Fichtner et al., 2013] and phase velocity for that model directly changes our estimate of transverse acceleration. Thus the quality of our results hinges on this Earth model. But it is hard to believe that phase velocity can be different by more than 10 percent. Also despite the concerns in Widmer-Schnidrig and Zuern [2009], the quality of the ring laser data after (mid-) 2009 is substantially improved [Hadziioannou et al., 2012] and a faithful recording of small-amplitude waves by such ring laser systems is not a problem at all now [e.g., Igel et al., 2011]. Therefore, our results indicate that there is at least comparable Love wave energy with Rayleigh wave energy in the secondary microseism and it is very likely that Love-wave energy exceeds Rayleigh-wave energy.

Using Rayleigh wave phase velocity for the seismic model and our spectral amplitude observations, we can estimate the effect of tilt directly. Tilt can be estimated by $|\partial u_z / \partial x| \sim |ku_z| \sim |\mathrm{v}_z / \mathrm{C}| \sim |1.6 \times 10^{-9} / 3200| \sim 5.0 \times 10^{-13}$, where v_z is velocity and the maximum peak in Fig. 2 is used for its estimate. Also phase velocity C=3200 m/s is used. The peak rotation rate from the ring laser is 3×10^{-13} (rad/s) (Fig. 2 is in nano radians). The main contamination source in this case is the projection of the Earth's rotation rate because of tilt. Using equation (17) in Pham et al. [2009], we get the fractional contribution of tilt is $(5 \times 10^{-13} \times 7.27 \times 10^{-5} / 3 \times 10^{-13}) \sim 1.2 \times 10^{-4}$ or 0.012 percent. This is negligible for this study.

Our result is an estimate at a single location (WET). But as seismic noise consists of propagating surface waves, our estimate for Rayleigh waves and Love waves should apply to broader regions.

Our result makes a contrast to a result in Nishida et al. [2008]. Their result indicated that Love-wave energy is about 50 percent of Rayleigh-wave energy above 0.1 Hz, although Love-wave energy is larger for frequencies below 0.1 Hz. Because our data and approaches are different, it is hard to pinpoint the cause of this difference but we believe there is a possibility such Love to Rayleigh wave ratios may be different in Japan from the European continent. But resolution of this question requires more careful study for each region. On the other hand, it is important to note that both studies show that Love-wave energy is quite high in the microseisms.

Our conclusion clearly poses a challenge to our understanding of the excitation mechanism of the secondary microseism. The Longuet-Higgins mechanism, the wave-wave interactions of ocean waves [Longuet-Higgins, 1950], is generally accepted to be the main mechanism of excitation but because it is essentially equivalent to a vertical force, it only excites Rayleigh waves in a layered medium. Even in the real Earth, it cannot be an efficient source to excite Love waves. A similar conundrum applies to the toroidal hum whose source is not understood (e.g., Kurrle and Widmer-Schnidrig, 2008).

Conversion from Rayleigh waves to Love waves is certainly possible at ocean-continent boundaries, but can it lead to a situation with comparable or more Love-wave energy than Rayleigh-wave energy? Our results seem to require careful rethinking of Love-wave excitation in the frequency band of the secondary microseism.

Acknowledgments

All data used in this study, ring laser data and STS-2 data at WET, are available from the GEOFON and EIDA data archives at www.webdc.eu. The operation of the ring laser is supported by the Bundesamt für Kartographie und Geodäsie (BKG). HI acknowledges support from the ERC Advanced Grant "ROMY", CH from grant HA7019/1-1 by the Emmy-Noether Programme of the German Research Foundation (DFG), and US and AG from grant Schr645/6-1 by the DFG. TT is grateful for a fellowship from the Center for Advanced Study at LMU, Munich. We thank M. Afanasiev and A. Fichtner for the seismic model at WET and Dr. Walter Zuern and an anonymous reviewer for comments.

References

Chevrot, S., M. Sylvander, S. Benahmed, C. Ponsolles, J. M. Lefe`vre, and D. Paradis (2007), Source locations of secondary microseisms in westernEurope: Evidence for both coastal and pelagic sources, J Geophys. Res., 112, B11301, doi:10.1029/2007JB005059

Ferreira, A. and I. Igel (2009), Rotational motions of seismic surface waves in a laterally heterogeneous Earth, Bull. Seism. Soc. Am., 99(2B), 1429-1436.

Fichtner, A., J. Trampert, P. Cupillard, E. Saygin, T. Taymaz, Y. Capdeville and A. Villasenor (2013), Multiscale full waveform inversion, *Geophys. J. Int.,* 194, 534-556, doi:10.1093/gji/ggt118

Hadziioannou, C., P. Gaebler, U. Schreiber, J. Wassermann, and H. Igel (2012), Examining ambient noise using co-located measurements of rotational and translational motion, *J. Seismol*., **16**, 787, doi:10.1007/s10950-012-9288-5.

Igel, H., U. Schreiber, A. Flaws, B. Schuberth, A. Velikoseltsev, and A. Cochard (2005), Rotational motions induced by the M8.1 Tokachioki earthquake, September 25, 2003, *Geophys. Res. Lett.,* 32, L08309, doi:10.1029/2004GL022336.

Igel H, Cochard A, Wassermann J, Flaws A, Schreiber U, Velikoseltsev A, Pham Dinh N (2007) Broad-band observations of earthquake-induced rotational ground motions, *Geophys. J Int.,* 168(1):182–196

Igel, H., M-F. Nader, D. Kurrle, A-M. G. Ferreira, J. Wassermann, and K. U. Schreiber (2011), Observations of Earth's toroidal free oscillations with a rotation sensor: The 2011 magnitude 9.0 Tohoku-Oki earthquake, *Geophys. Res. Lett*. **38**, L21303, doi:10.1029/2011GL049045

Kurrle, D. and R. Widmer-Schnidrig (2008). The horizontal hum of the Earth: a global background of spheroidal and toroidal modes, *Geophys. Res. Lett.,* **35**(6), L06304, doi:10.1029/2007GL033125.

Kurrle, D., H. Igel, A-M. G. Ferreira, J. Wassermann, and U. Schreiber (2010), Can we estimate local Love wave dispersion properties from collocated amplitude measurements of translations and rotations?, *Geophys. Res. Lett*., **37**(4), 1, doi:10.1029/2009GL042215

Longuet-Higgins, M. (1950), A theory of the origin of microseisms. *Phil. Trans. R. Soc. Lond., Ser A*, *Math. Phy.s Sci.,* 243(857), 1–35.

Nishida K, Kawakatsu H, Fukao Y, Obara K (2008) Background Love and Rayleigh waves simultaneously generated at the Pacific Ocean floors, *Geophys. Res. Lett.,* 35(16):1–5

Pancha A., T.H. Webb, G. E. Stedman,D. P. McLeod, and K. U. Schreiber (2000), Ring laser detection of rotations from teleseismic waves, *Geophys Res Lett* 27(21):3553

Pham N., H. Igel, J. Wassermann, Kaser M, de La Puente J, Schreiber U (2009) Observations and modeling of rotational signals in the P-coda: constraints on crustal scattering, *Bull. Seism. Soc. Am.,* 99(2B):1315

Schreiber, U., and J.-P. Wells (2013), Invited Review Article: Large ring laser for rotation sensing, *Rev. Sci. Instrum*., 84, 041101, doi:10.1063/1.4798216

Schreiber, U., J. N. Hautmann, A. Velikoseltsev, J. Wassermann, H. Igel, J. Otero, F. Vernon, and J.‐P. R. Wells (2009), Ring laser measurements of ground rotations for seismology, *Bull. Seism. Soc. Am.,* 99(2B), 1190–1198, doi:10.1785/0120080171

Widmer-Schnidrig, R., and W. Zürn (2009), Perspectives for ring laser gyroscopes in low-frequency seismology. *Bull. Seism. Soc. Am.,* 99(2B):1199

Figure Captions

Fig. 1. **(Top-Left)** Power Spectral Density (PSD) of rotation rate (0.13-0.30 Hz), recorded by the ring laser at Wettzell. Each point was computed from a 6-hour long time series. Unit is nano-radians^2 /sec. Data from 2009 to 2014 are plotted, folded onto one year using the Julian day. Note that all energy is shear (SH). **(Top-Right)** Monthly means and the standard deviations from the left panel are shown, indicating amplitude variations of about 10 between summer and winter. **(Bottom)** WET is denoted by the red mark and close to the Germany-Czech border.

Fig. 2: **(Top)** Stacked spectral amplitudes of STS-2 from the vertical component (black), the north-south component (blue) and the east-west component (red). The two horizontal components basically overlap. **(Bottom)** Stacked spectral amplitudes from the ring laser (rotation) data. Large earthquake days were removed from stacking and exactly the same time intervals were used for computing both spectra.

Fig. 3: **(a)** Seismic model at WET from Fichtner et al. [2013]. Anisotropic P waves (PV and PH) and S waves (SV and SH). **(b)** Phase velocities of fundamental-mode Love waves. **(c)** Ellipticity of Rayleigh-wave particle motion at the surface. This ratio is used to estimate Rayleigh wave horizontal amplitudes at the surface.

Fig. 4: **(a)** Comparison among the transverse acceleration from the rotation measurements (red), the vertical acceleration from STS-2 (blue) and the horizontal acceleration from the vertical acceleration plus theoretical surface ellipticity (green). **(b)** The Rayleigh/Love ratio of surface amplitudes (red) and the ratio of the kinetic energy (blue). **(c)** The eigenfunctions of Love (red) and Rayleigh waves (blue and green) at 0.22 Hz. They are used to estimate the kinetic energy.

WET Ring-Laser Rotation

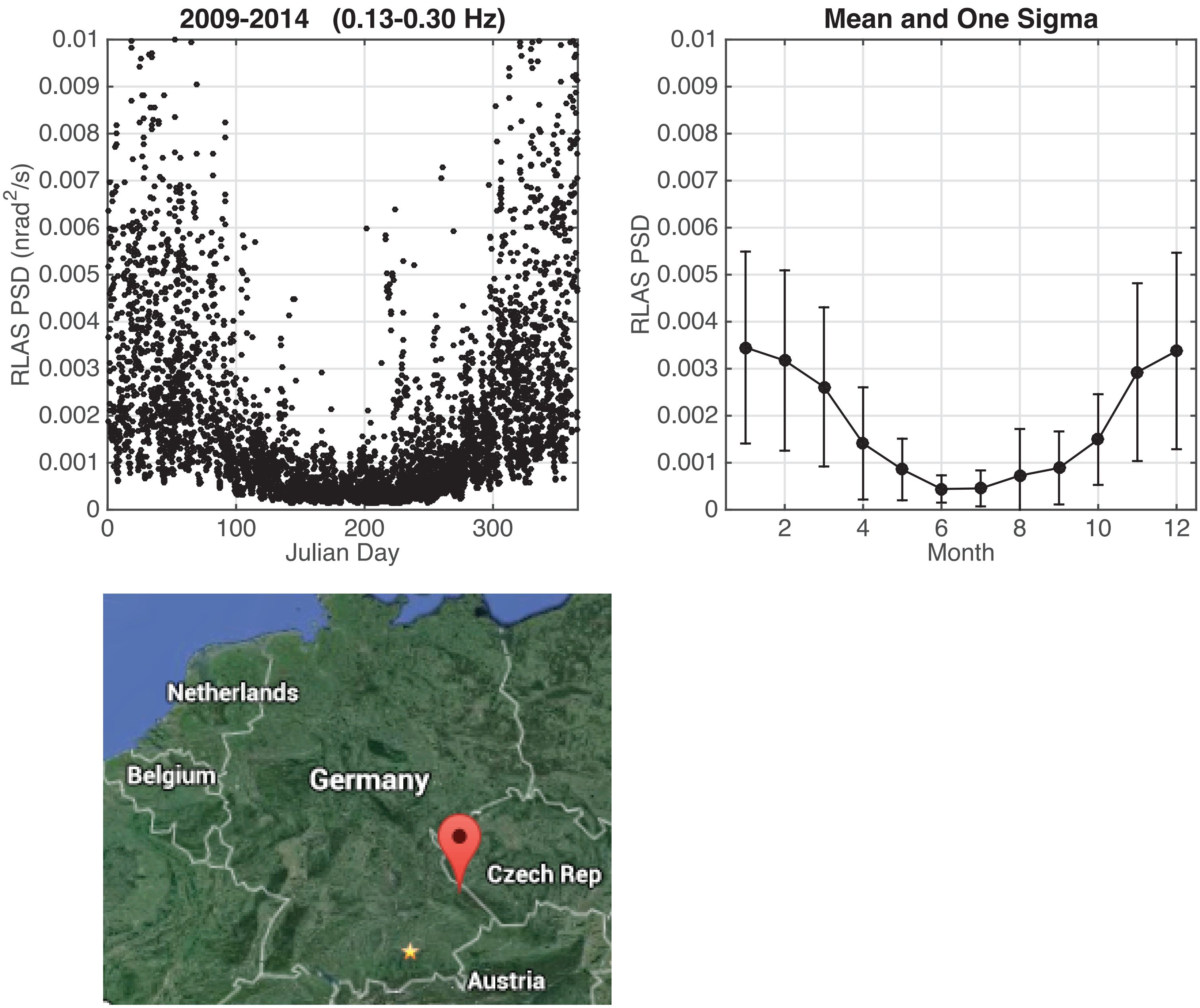

Figure 1

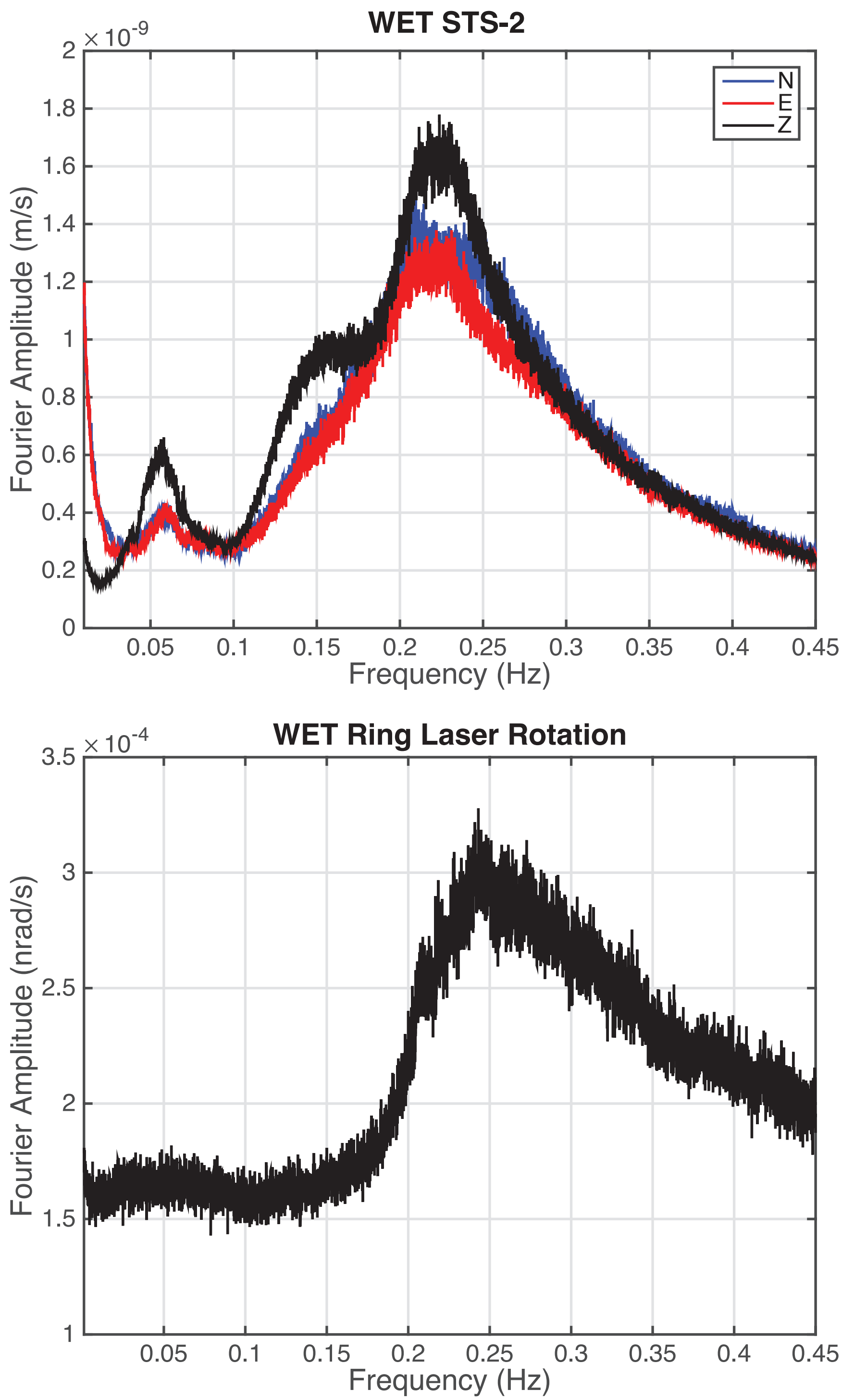
WET STS-2
× 10^-9
Fourier Amplitude (m/s)
Frequency (Hz)
N
E
Z
0
0.2
0.4
0.6
0.8
1
1.2
1.4
1.6
1.8
2
0.05
0.1
0.15
0.2
0.25
0.3
0.35
0.4
0.45
WET Ring Laser Rotation
× 10^-4
Fourier Amplitude (nrad/s)
Frequency (Hz)
1
1.5
2
2.5
3
3.5
0.05
0.1
0.15
0.2
0.25
0.3
0.35
0.4
0.45

Figure 2

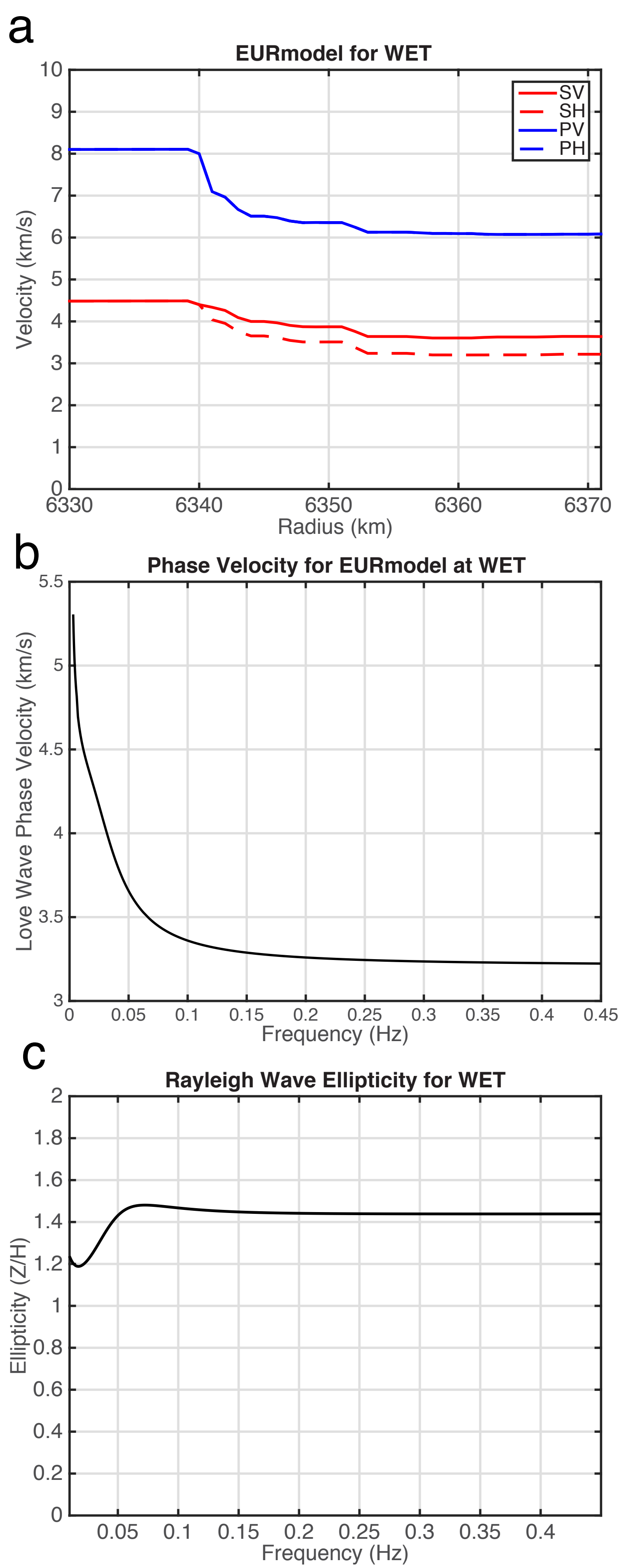

a
EURmodel for WET
SV
SH
PV
PH
Velocity (km/s)
Radius (km)
b
Phase Velocity for EURmodel at WET
Love Wave Phase Velocity (km/s)
Frequency (Hz)
c
Rayleigh Wave Ellipticity for WET
Ellipticity (Z/H)
Frequency (Hz)

Figure 3

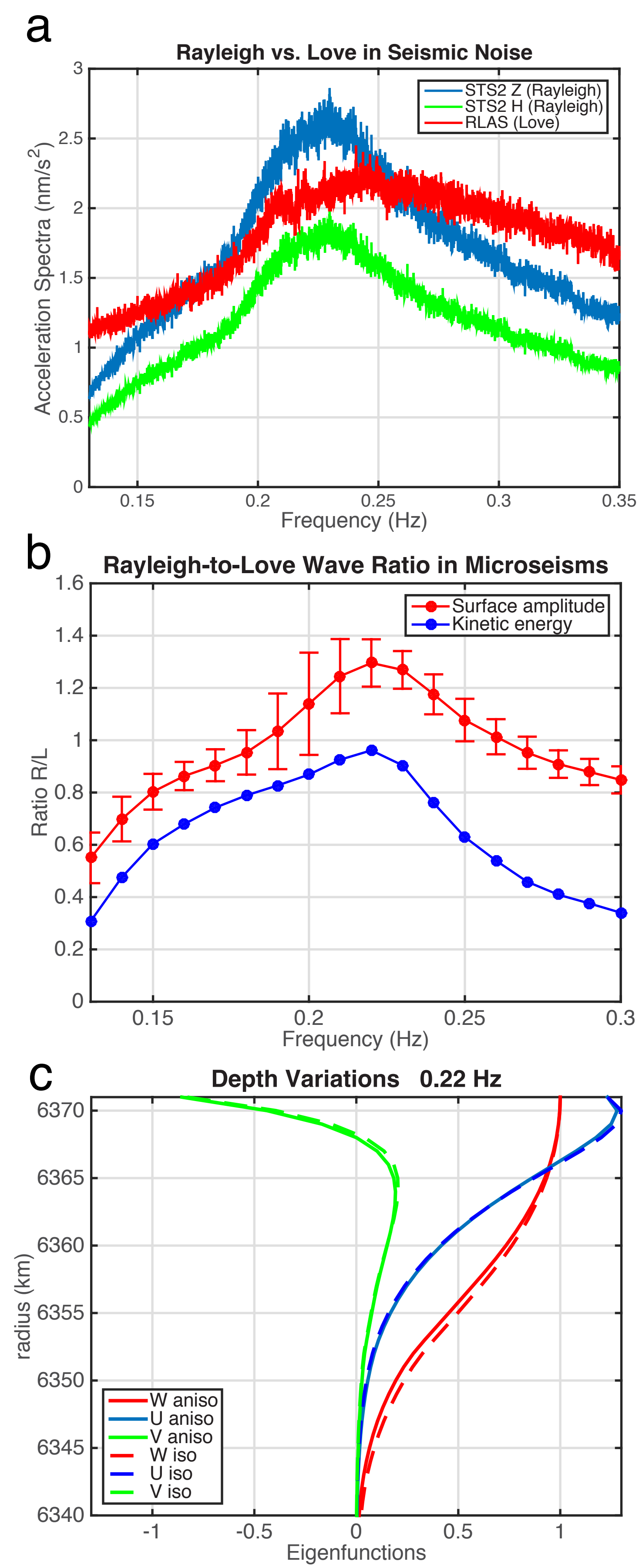
a
Rayleigh vs. Love in Seismic Noise
STS2 Z (Rayleigh)
STS2 H (Rayleigh)
RLAS (Love)
Acceleration Spectra (nm/s²)
Frequency (Hz)
b
Rayleigh-to-Love Wave Ratio in Microseisms
Surface amplitude
Kinetic energy
Ratio R/L
Frequency (Hz)
c
Depth Variations 0.22 Hz
radius (km)
W aniso
U aniso
V aniso
W iso
U iso
V iso
Eigenfunctions

Figure 4